J Solid State Electrochem (2010) 14:1163–1169
DOI 10.1007/s10008-009-0953-8

ORIGINAL PAPER

Stripping chronopotentiometric analysis of cysteine on nano-silver coat polyquercetin–MWCNT modified platinum electrode

Guan-Ping Jin · Li-Li Chen · Guo-Pei Hang · Shan-Zhong Yang · Xiao-Jing Wu

Received: 15 May 2009 / Revised: 13 July 2009 / Accepted: 7 October 2009 / Published online: 20 October 2009

Abstract Silver nanoparticles coat polyquercetin (Qu) and multi-walled carbon nanotube (MWCNT) complex films were prepared using an electrochemical coupling strategy on platinum electrode (Ag/Qu/MWCNT/Ch/Pt). The new composite material was characterized by means of field emission scanning electron microscopy, X-ray photoelectron spectroscopy spectra, X-ray diffraction, and electrochemical techniques, which confirmed that polyquercetin plays an important role to obtain a great deal of uniformly dispersed silver nanoparticles and MWCNT complex film with a diameter of 10±6 nm. The resulting Ag/Qu/MWCNT/Ch/Pt electrode shows a significant electrocatalysis for the redox of cysteine (CysH). The stripping chronopotentiometric analysis of CysH has been successfully used with a satisfying effect. A linear range of 1×10^{-10} to 9×10^{-8} M was obtained with a detection limit of 3×10^{-11} M (3σ) and sensitivity of 35 μA/nM. The films were also robust, surviving up to 100 consecutive cyclic voltammograms and sonication.

Keywords Stripping chronopotentiometric analysis · CysHteine · Silver nanoparticles · Multi-walled carbon nanotube

G.-P. Jin · L.-L. Chen · X.-J. Wu
Anhui Key Laboratory of Controllable Chemistry Reaction & Material Chemical Engineering, School of Chemical Engineering, Hefei University of Technology,
Hefei 230009, People's Republic of China

G.-P. Jin (✉) · L.-L. Chen · G.-P. Hang · S.-Z. Yang · X.-J. Wu
Department of Application Chemistry of School of Chemical Engineering, Hefei University of Technology,
Hefei 230009, People's Republic of China
e-mail: jgp@hfut.edu.cn

Introduction

Cysteine (CysH) is a physiologically active substance which always exists in many kinds of protein and natural substances. It plays an important role in biological systems including protein synthesis, detoxification, and metabolism [1, 2]. It has been used widely in the food, cosmetic, and medical industries [3]. The studies that focused on the electrochemical behaviors and sensitive detection of CysH are significant from the viewpoints of theory and practical application. The electrochemical oxidation of CysH on various electrodes including graphite [2], platinum, and gold, especially silver, have been reported [4–9]. The adsorption of CysH at silver (Ag) electrode [7–9] involved the scheme of Ag (s) + CysH (ac) → Ag–Cys (ad) + H^+ (ac) + e^-. However, the high oxidation potential of CysH at these electrodes causes the formation of surface oxide with slow heterogeneous electron transfer, resulting in a dramatic decrease in electrochemical activity. Some improvements have been achieved by modifying the electrode with enzyme [3, 10], metal complexes [10–18], and organic compounds [19–22], but the stability of such modified electrodes was not satisfaction [12]. Recently, nanometal [23], MWCNT [24–26], and their complex modified electrodes [27] have attracted an increasing attention to improve the electrocatalysis. Chen J.H. successfully used nano-platinum/MWCNT modified electrode in CysH detection; the complex electrode displayed a better stability and reproducibility compared with only nano-platinum or MWCNT electrode [24, 27], but there is possibility in the improvement of sensitivity and detection limit.

In a previous work, we have investigated the preparation of highly dispersed nano-Ag/polyrutin coat–paraffin-impregnated graphite electrode. The studies showed that Ag^+ was gradually chelated with polyrutin film at 4′-oxo-5′-OH

and 5-OH-4-oxo sites accompanying adsorption [28]. Here, we used quercetin, the homolog of rutin, fabricated nano-Ag, polyquercetin, and MWCNT complex modified platinum electrode (Ag/Qu/MWCNT/Ch/Pt) to develop a sensitive sensor for CysH. The electrochemical behavior of CysH was investigated in detail.

Experimental

Apparatus

All electrochemical experiments were performed with a LK98BII computer electric chemistry analysis system (Lanlike, Tianjin, China). A conventional three-electrode electrochemical system was used for all electrochemical experiments, which consisted of a working electrode, a twisted platinum wire counter electrode, and a reference electrode. A platinum electrode with geometric diameter of 0.4 mm was used as the basal working electrode. Water used in all experiments was double-distilled with a quartz apparatus. Field emission scanning electron microscopy (FE-SEM) image was obtained on a JSM-600 field emission scanning electron microanalyzer (JEOL, Japan). X-ray photoelectron spectroscopy (XPS) spectra were recorded by using an ESCALAB MK_2 spectrometer (Vg Corporation, UK) with an Mg-Alpha X-ray radiation as the source for excitation. X-ray diffraction (XRD) data of the sample were collected using a Rigaku D/MAX-rB diffractometer with CuKα radiation.

Chemicals and solutions

MWCNT with diameters of 10–30 nm and lengths of 1–10 μm were purchased from Sun Nanotech Co., Ltd. of China, and were synthesized by catalytic decomposition of CH_4 on a NiMgO catalyst [28]. CysH and Qu were purchased from Xinxing Chemical Reagent Institute (Shanghai, China); solutions of CysH were prepared in 0.1-M PBS (pH 3.0). Phosphate-buffered saline solutions (0.1 M PBS) of different pH were prepared by mixing four stock solutions of 0.1 M H_3PO_4, KH_2PO_4, K_2HPO_4, and K_3PO_4. All aqueous solutions were prepared in doubly distilled deionized water. High-purity nitrogen was used for deaeration. All experiments were performed at room temperature.

Preparation of Ag/Qu/MWCNT/Ch/Pt electrode

The 10 mg MWCNT were dispersed in 10 ml of mixed acid solution of nitric acid and perchlorate acid (7:3). The mixed solution was ultrasonically agitated for 7 h. The MWCNT were washed with doubly distilled water to a neutral pH, then washed with acetone and dried in air. About 2.5 mg of mixed acid-treated MWCNT was dispersed in 10 ml of acetone with the aid of ultrasonic agitation to give 0.25 mg ml^{-1} black suspension.

Prior to this experiment, Pt electrode was polished with fine emery paper (grain size 4,000) and 0.03 μm Al_2O_3 powders to obtain a mirror surface. Then it was rinsed with doubly distilled water and sonicated in ethanol and doubly distilled water for 5 min, respectively. After cleaning, the Pt electrode was pretreated using cyclic voltammetry (CV) in solution of 1.0×10^{-3} M choline ($HOCH_2CH_2N^+(CH_3)_3$)/0.01 M $LiClO_4$ to obtain a film with positive charge (Ch/Pt) [29].

Some mixed acid-treated MWCNT solution were cast onto the surface of Ch/Pt by electrostatic adsorption (MWCNT/Ch/Pt). After the solvent acetone was evaporated, Qu was polymerized on the MWCNT/Ch/Pt using the CV method in a solution of 1×10^{-3} M Qu/0.1 M PBS (pH 7.0; Qu/MWCNT/Ch/Pt). Some Ag^+ was chelated or absorbed on the surface of Qu/MWCNT/Ch/Pt immersed in a solution of 1.0×10^{-3} M $AgNO_3$/0.1 M $LiNO_3$ in 30 min, then, the complex was reduced in blank 0.1 M $LiNO_3$. The modified electrode was denoted as Ag/Qu/MWCNT/Ch/Pt and stored in doubly distilled water at 4 °C.

Results and discussion

The characteristics of Ag/Qu/MWCNT/Ch nanocomposite

Figure 1 shows FE-SEM images of Ag/MWCNT/Ch/Pt (Fig. 1a), Ag/Qu/MWCNT/Ch/Pt made by directly electrodepositing in 1.0×10^{-3} M $AgNO_3$/0.1 M $LiNO_3$ (Fig. 1b) and by immersing in 1.0×10^{-3} M $AgNO_3$/0.1 M $LiNO_3$ for 30 min, then, reducing in blank 0.1 M $LiNO_3$ (Fig. 1c). In absence of Qu by direct electrodeposition, numerous larger dendritic clusters can be seen with a strong aggregate effect in 3-dimensional globules (Fig. 1a). It is relative to an advantageous effect of MWCNT with carboxylic acid and carboxylate groups towards the deposition of Ag^+ and resulting in spontaneous formation of Ag nanoparticles on MWCNT. However, as shown in Fig. 1b, a great deal of uniformly dispersed island structures can be seen with a diameter of 50±30 nm on the surface of Qu/MWCNT/Ch/Pt by directly electrodepositing because the polyquercetin can chelate (absorb) Ag^+ and result in a slow mass transition. Furthermore, after the Qu/MWCNT/Ch/Pt was immersed in 1.0×10^{-3} M $AgNO_3$/0.1 M $LiNO_3$ in 30 min to chelate (absorb) Ag^+, the complex was reduced in blank 0.1 M $LiNO_3$; a much better effect can be readily seen with a diameter of 10±6 nm. Therefore, these illustrate that the polyquercetin plays an important role to obtain the uniformly dispersed nanocomposite; the result is very significant for practical application. The processes can be seen in Scheme 1.

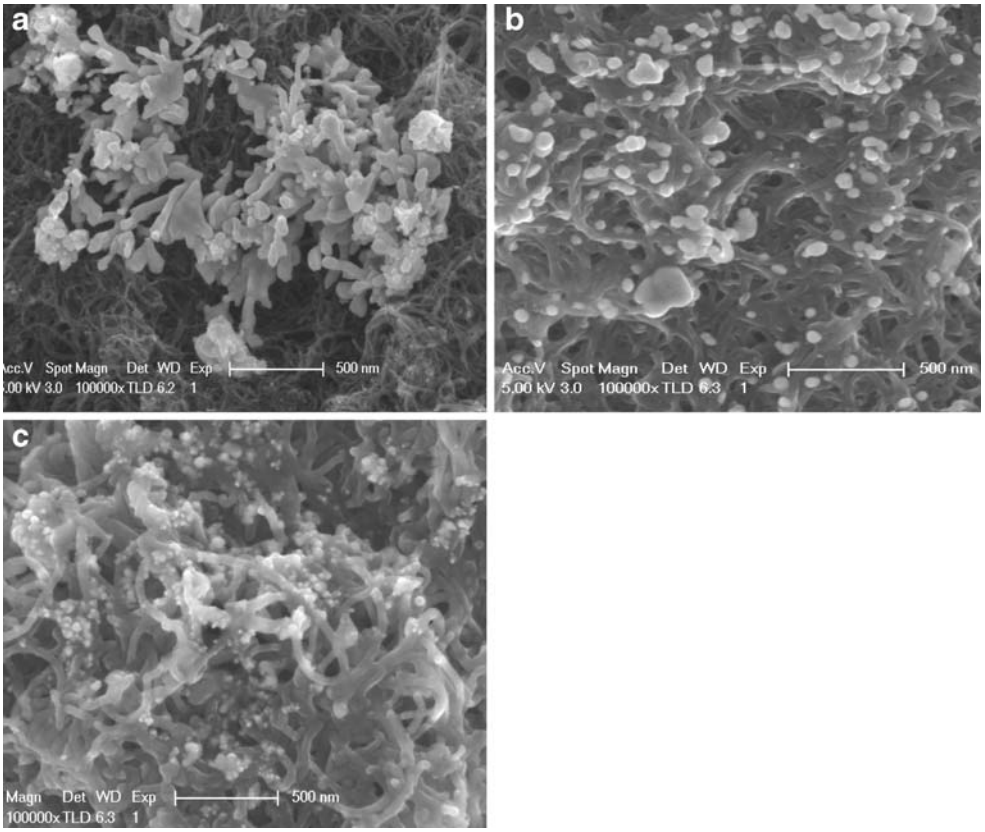

Fig. 1 FE-SEM of Ag/MWCNT/Ch (**a**), Ag/Qu/MWCNT/Ch made by directly electrodepositing in 1.0×10^{-3} M $AgNO_3$/0.1 M $LiNO_3$ (**b**), and by immersing in 1.0×10^{-3} M $AgNO_3$/0.1 M $LiNO_3$ for 30 min, then, reducing in blank 0.1 M $LiNO_3$ (**c**)

The XRD of the nanocomposite formed by indirect electrodepositing was investigated and is shown in Fig. 2. The MWCNTs showed a typical peak of (002) reflection of MWCNT or graphite at 26.34 °C. The major diffraction peaks of Ag nanoparticles at 37.2 °C and 44. 2 °C can be assigned to (111), (200) reflection of fcc phase of Ag. The size of 10±6 nm was derived according to Scherrer formula formed. It illustrates that Qu can improve the surface

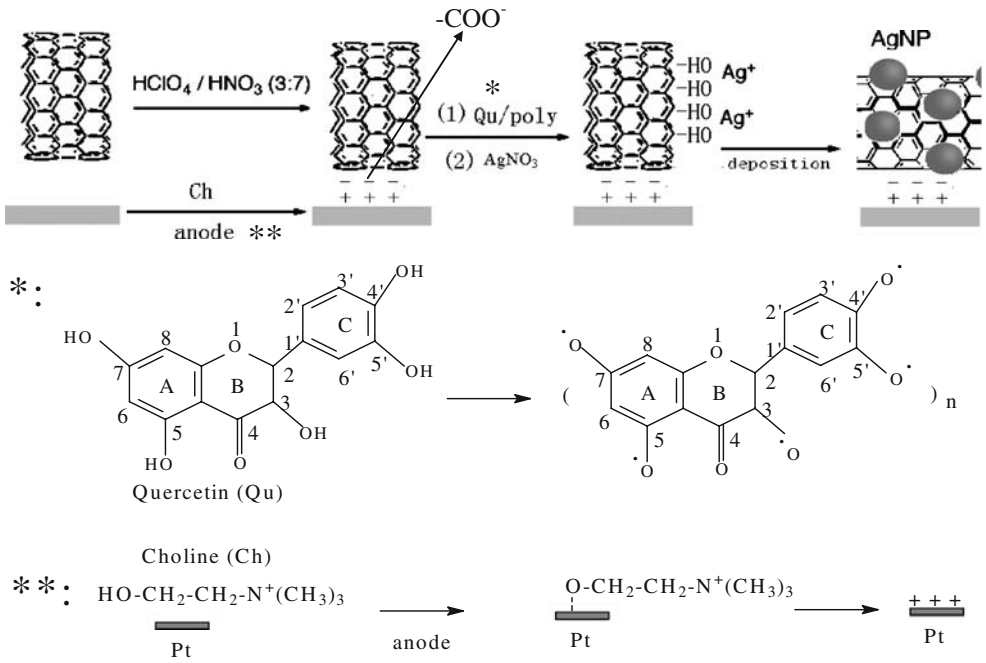

Scheme 1 Synthesis of nano-silver coat polyquercetin and multi-walled carbon nanotube complex films

morphology and diminish the nano-Ag size [28]. XPS measurements confirmed the presence of Ag on the Ag/Qu/MWCNT/Ch/Pt after electrochemical immobilization. The Ag ($3d_{5/2}$) and Ag ($3d_{3/2}$) peaks are present at 368.6 and 374.6 eV, respectively (Fig. 2, inset).

Electrochemical behaviors of CysH at Ag/Qu/MWCNT/Ch/Pt

As shown in Fig. 3, from 1.4 → −0.4 V, Pt electrode (a) shows two reduction peaks (−0.20 and 0.10 V) and one oxidation peak (0.75 V) corresponding to hydrogen and oxygen adsorbed on Pt, respectively [30]. MWCNT/Ch/Pt (b) displays a pair of peaks of oxygen adsorbed on MWCNT (0.12/0.22 V) [29]. Qu/MWCNT/Ch/Pt (c) gives same peaks to Pt electrode. However, Ag/Qu/MWCNT/Ch/Pt (d) gives one new reduction peak at 0.04 V and three new oxidation peaks at 0.12, 0.23, 0.50 except above peaks, which could match to the process of $Ag \rightarrow Ag_2O \rightarrow AgO$ [31, 32]. The surface area of Ag/Qu/MWCNT/Ch/Pt can be evaluated as 0.456 cm^2 from charge current; all the Ag anode peak surface area is 0.043 μC. From Faraday law, a surface concentration (Γ) of the Ag was calculated as 9.4×10^{-8} M/cm^2. According to the facts, the modification can be suggested in Scheme 1. The Pt electrode was pretreated in a solution of choline (+) to adsorb MWCNT (−); after quercetin was polymerized on the MWCNT/Ch/Pt to chelate or absorb Ag^+, the complex with Ag^+ was reduced to obtain silver nanoparticles/polyquercetin (Qu)/multi-walled carbon nanotube complex films (Ag/Qu/MWCNT/Ch/Pt).

Figure 4 shows the CVs of 1.0×10^{-4} M CysH (curve b) at bare Pt (A), MWCNT/Ch/Pt (B), and Ag/Qu/MWCNT/Ch/Pt (C), respectively. All the curves (a) have been

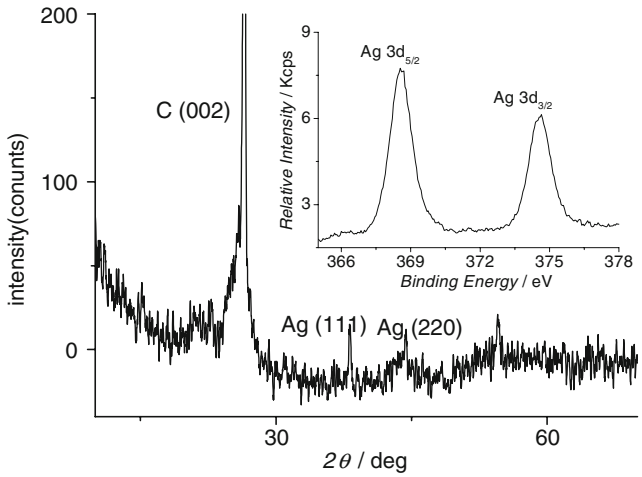

Fig. 2 XRD and XPS (*inset*) of Ag/Qu/MWCNT/Ch (preparation is same to Fig. 1c)

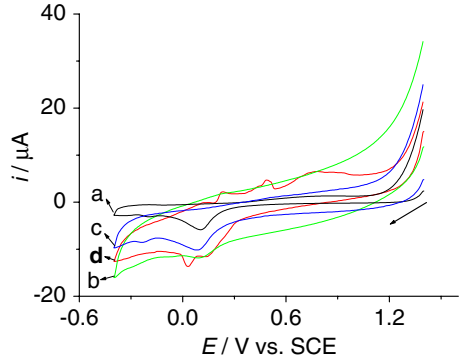

Fig. 3 CVs of Pt electrode (*a*), MWCNT/Ch/Pt (*b*), Qu/MWCNT/Ch/Pt (*c*), and Ag/Qu/MWCNT/Ch/Pt (*d*). Scan rate: 50 mVs^{-1}. Buffer: 0.1 M PBS (pH 3.0)

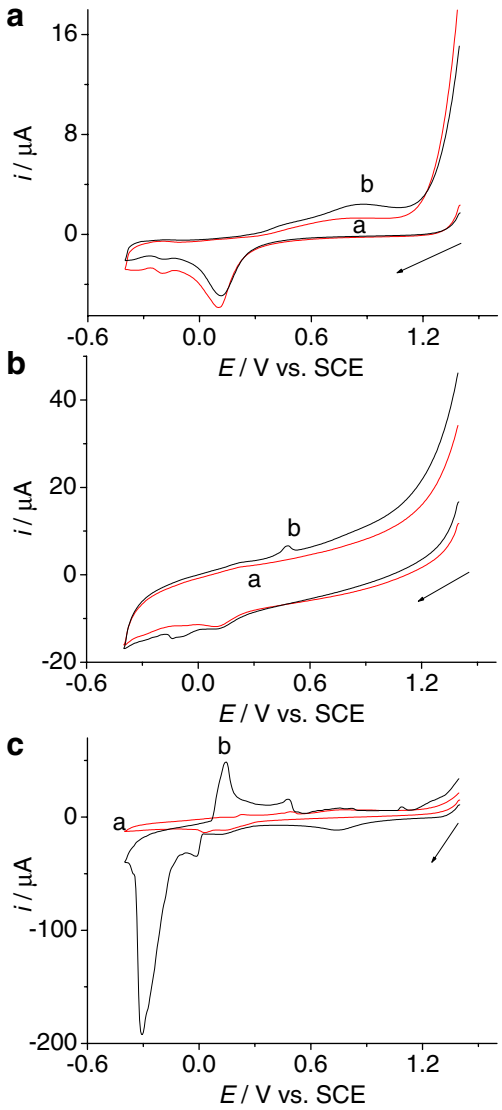

Fig. 4 CVs of Pt electrode (*a*), MWCNT/Ch/Pt (*b*), and Ag/Qu/MWCNT/Ch/Pt (*c*) in absence (*a*) and presence (*b*) of 1.0×10^{-4} M CysH. Accumulation time: 60 s. Accumulation potential: 0.5 V. Scan rate: 50 mVs^{-1}. Buffer: 0.1 M PBS (pH 3.0)

Table 1 The response of 1.0×10^{-4} M cysteine at different electrodes

Sample/ electrode	Pt	Ch/Pt	Ag/Pt	MWCNT/ Ch/Pt	Qu/MWCNT/ Ch/Pt	Ag/Qu/ MWCNT/Ch/Pt
Reduction peak current (μA)	1.25	1.26	85.25	2.14	1.11	165.45
Rate (electrode/ Pt)		1.0	68.2	1.6	0.8	132.3

discussed in Fig. 3 matching to the electrodes in blank PBS. The oxidation current of CysH (0.85 V) is decreasing dramatically because the active sites of Pt are blocked by adsorption of reaction products including cystine acid and cysteic acid at bare Pt electrode (Fig. 4a, curve b) [27, 29, 33]. On the MWCNT/Ch/Pt electrode (Fig. 4b, curve b), this problem can be reduced successfully by using a low potential at about 0.46 V. It was confirmed that the oxidation current of CysH decreased very little in the 2nd cycle and remains almost unchanged from the 2nd to the 10th cycle in the potential range of −0.5 to 0.7 V (not shown). But the

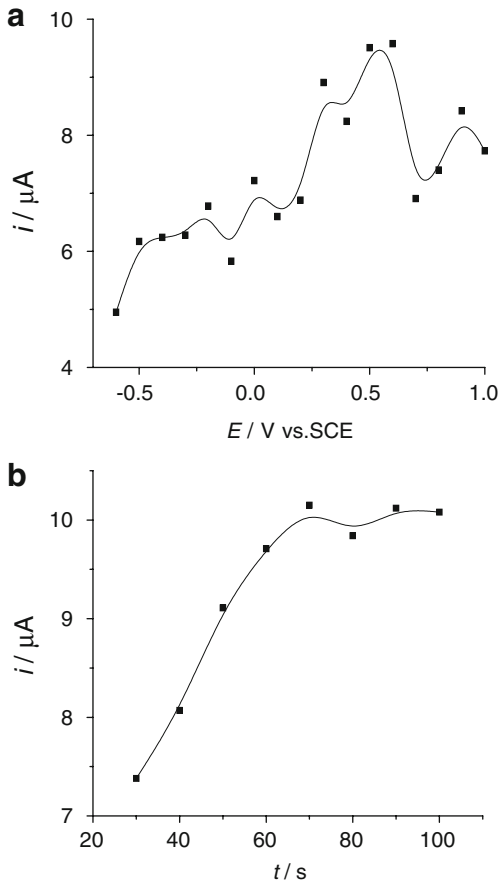

Fig. 5 **a** The oxidation peak currents of 1.0×10^{-4} M CysH (0.13 V) depend on the potential with accumulation time of 60 s. **b** The oxidation peak currents of 1.0×10^{-4} M CysH (0.13 V) depend on the accumulation time at 0.5 V. Scan rate: 50 mVs^{-1}. Buffer: 0.1 M PBS (pH 3.0)

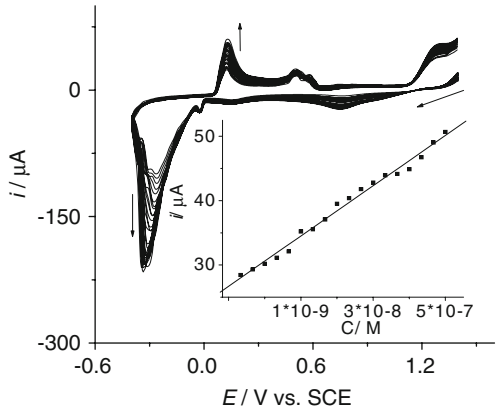

Fig. 6 The CVs of CysH depend on the concentration. *Inset*: reduction peak currents (0.13 V) of CysH depend on the concentration. Accumulation potential: 0.5 V. Accumulation time: 60 s. Scan rate: 50 mVs^{-1}. Buffer: 0.1 M PBS (pH 3.0)

sensitivity and detection limits still can be improved. As shown in the Fig. 4c, in the presence of CysH (curve b), all the peaks are observed to be obviously increase at Ag/Qu/MWCNT/Ch/Pt with slightly negative shift in potential compared with in absence of CysH (curve a). The increase of the peak's current at −0.30 and 0.13 V are significantly stronger than that at other electrodes. Moreover, the CVs of 1.0×10^{-4} M CysH at Ch/Pt, Ag/Pt, and Qu/MWCNT/Ch/Pt were also performed in the same conditions; the results were summarized in Table 1. The present data prove that MWCNT/Ch/Pt, Ag/Pt, and Ag/Qu/MWCNT/Ch/Pt shows significant increase by degrees effect towards the redox of CysH. Therefore, the Ag/Qu/MWCNT/Ch/Pt electrode shows an excellent electrocatalysis towards the redox of CysH. The processes probably involve alternative process; a vital one is desorption/adsorption of CysH at Ag/Qu/MWCNT/Ch/Pt accompanying the production of Ag^{+}, the partially unsaturated d-orbital of Ag atom surface could absorb and thereby stabilize free radical intermediate of the oxidation products of CysH. The Ag nanoparticles can

Table 2 Determination limits of CysH at different modified electrodes

Modification	Limits (μM)	Reference
Poly(3,4-ethylenedioxythiophene)/SPE	0.03	[22]
Ru-complex/GCE	1	[16]
N,*N*-ethylene*bis* oxovanadium/GCE	170	[17]
Bi-powder/CPE	0.3	[18]
Co-tetra-2-mercaptopyrimidylphthalocyanine/ GCE	1.5	[14]
MWCNT/GCE	5.4	[24]
Mercury-doped/Ag/GCE	0.1	[23]
Pt/MWCNT/CPE	0.3	[27]
Ag/Qu/MWCNT/Ch/Pt	0.00003	This work

GCE Glassy carbon electrode, *CPE* carbon paste electrode, *SPE* screen-printed electrode

further oxidize the oxidation products of CysH at a low potential. The other is relative to cooperation of MWCNT towards the redox of CysH.

Stripping chronopotentiometric analysis

The effect of accumulation potential (E) towards CysH (0.13 V) was investigated at Ag/Qu/MWCNT/Ch/Pt and shown in Fig. 5a. The concentration of Ag^+ is increasing with the positive shift of accumulation potential. The peak current is low at $E<-0.5$ V due to a little production of Ag^+; the response is slowly increasing in -0.6 V$<E<0.25$ V and considerable increase in 0.25 V$<E<0.60$ V. It reaches the largest in $0.5\leq E\leq 0.60$ V, implying an optimum accumulation potential. But, the response is decreasing at $E>0.6$ V; the reason could be relative to the superfluous and fast production of Ag^+ can form insoluble salt with CysH [9].

The effect of accumulation time towards CysH (0.13 V) was investigated at Ag/Qu/MWCNT/Ch/Pt at 0.5 V. As shown in Fig. 5b, the peak current (0.13 V) is quickly increasing with the delay of time, then, reaches a flat roof at time >60 s, implying an adsorption balance. The optimal accumulation time is 60 s (response time). Moreover, the response of CysH (0.13 V) was investigated with the variety of pH. The peak potential only shows slight negative shift with the increase of pH. The reduction peak at −0.3 V and oxidation peak at 0.13 V are stronger at pH 3 and pH 2, and all the peaks can be well separated at pH 3, thus, the suitable pH value is 3.0.

As a comparison, the only Ag electrode is investigated towards the redox of CysH, too. The peak current rate (about 0.13 V) of Ag electrode is 1.5 in the presence and absence of 0.1 mM CysH. The rate is 2.9 at Ag/Qu/MWCNT/Ch/Pt in a same situation. It illustrated that the Ag/Qu/MWCNT/Ch/Pt shows a much better electrocatalysis towards CysH.

As shown in Fig. 6, on the optimal conditions, the peak currents at 0.13 V show a good linearity in a concentration range of 1×10^{-10}–5×10^{-7} M ($i(\mu A)$=26.7+1.3 C (M), R= 0.9941; $LOD=3\times10^{-11}$ M (3σ); SOD, 1.3%, n=5; sensitivity, 15 μA/nM; inset). The peak at −0.30 displays a good linear increase in the concentration ranges of 1×10^{-10} to 9×10^{-8} M ($i(\mu A)$=68.9+5.0 C (M), R=0.9931; $LOD=1\times10^{-11}$ M (3σ); SOD, 1.1%, n=5; sensitivity, 35 μA/nM). Moreover, in comparison with the results of Table 2, their detection limits are 1.5, 1, 170, 0.3, 0.03, 0.1, 5.4, and 0.3 μM, respectively; therefore, the present electrode shows the lowest detection limit. Moreover, it is notable that the films were also robust, surviving up to 100 consecutive cyclic voltammograms and sonication.

The interference effects of 18 amino acids including glycine, alanine, valine, leucine, isoleucine, serine, threonine, tyrosine tryptophan, methionine, asparagines, glutamine, glutamic acid, lysine, aspartic acid, arginine, phenylalanine, histidine, and proline to the determination of CysH were investigated due to coexistence in biological samples. The results show that any one (100 times content) of the 18 amino acids did not interfere determination of CysH except 20 times tyrosine and 20 times tryptophan (the peaks at about 0.6 V). It is worth mentioning that the presence of 2, 5, 10, 10, 10, 20, and 5 times content of glutathione, homocysteine, dopamine, norepinephrine, adrenalin, ascorbic acid, and uric acid positively interferes the determination, respectively.

Conclusion

In summary, we have demonstrated a method to prepare uniformly dispersed nano-silver and MWCNT coat platinum electrode (Ag/Qu/MWCVT/Ch/Pt). The electrode is advantageous for sensing of CysH compared with bare Pt, MWCNT/Pt, and Ag electrodes with satisfactory results. The method is simple and easy to control. Therefore, the approach may be useful for the synthesis of other hybrid metal/MWCNTs complex.

Acknowledgements We gratefully acknowledge financial support from 2010 Natural Science Foundation of Anhui Province Altitude School of China; Undergraduate Innovation Experiment Program (2009CXSY135) of Hefei University of Technology, Student Innovation Fund (200924) of Hefei University of Technology, and Doctor Foundation of Hefei University of Technology (2005).

References

1. Chen HL, Li MS (1999) Structure and function of biomacromolecules. Shanghai Science Press, Shanghai, pp 4–9
2. Reynaud JA, Maltoy B, Canessan P (1980) J Electroanal Chem 114:195
3. Pradac J, Koryta J (1968) J Electroanal Chem 17:185
4. Santhiago M, Vieira IC (2007) Sens Acutators B 128:279
5. Ca D, Sun LS, Cox JA (2006) Electrochim Acta 51:2188
6. Fawcett WR, Fedurco M, Kovácová Z, Borkowska Z (1994) J Electroanal Chem 368:265
7. Santos E, Avalle L, PÖtting K, Vélez P, Jones H (2008) Electrochim Acta 53:6807
8. Santos E, Avalle LB, Scurtu R, Jones H (2007) Chem Phys 342:236
9. Fang B, Fang HQ, Chen HY (1996) J Chin Univ 17:1384
10. Huang TH, Kuwana T, Warsinke A (2002) Biosens Bioelectron 17:1107
11. Maree S, Nyokong T (2000) J Electroanal Chem 492:120
12. Halbert MK, Baldwin RP (1985) Anal Chem 57:591
13. Amini MK, Khorasani JH, Khaloo SS, Tangestaninejad S (2003) Anal Biochem 320:32
14. Obirai JC, Nyokong T (2007) J Electroanal Chem 600:251
15. Mafatle TJ, Nyokong T (1996) J Electroanal Chem 408:213
16. Salimi A, Pourbeyram S (2003) Talanta 60:205
17. Teixeira MFS, Dockal ER, Cavalheiro ÉTG (2005) Sens Acutators B 106:619

18. Baldrianova, Svancara PA, Vytras K, Sotiropoulos S (2008) Electrochem Commun 10:918
19. Lima PR, Santos WJR, Luz RCS, Damos FS, Oliveira AB, Goulart MOF, Kubota LT (2008) J Electroanal Chem 612:87
20. Ardakani MM, Rahimi P, Karami PE, Zare HR, Naeimi H (2007) Sens Acutators B 123:763
21. Tong J, Nie MY, Li HL (1997) J Electroanal Chem 433:121
22. Su WY, Cheng SH (2008) Electrochem Commun 10:899
23. Li MG, Shang YJ, Gao YC, Wang GF, Fang B (2005) Anal Biochem 341:52
24. Salimi A, Hallaj R (2005) Talanta 66:967
25. Zhao YD, Zhang WD, Cheng H, Luo QM (2003) Sens Acutators B 92:279
26. Okuno J, Maehashi K, Matsumoto K, Kerman K, Takamura Y, Tamiya E (2007) Electrochem Commun 9:13
27. Fei S, Chen JH, Yao SZ, Deng GH, He DL, Kuang YF (2005) Anal Biochem 339:29
28. Jin GP, Peng X, Chen QZ (2008) Electroanalysis 20:907
29. Jin GP, Ding YF, Yin JG (2007) Chin J Chem 25:1
30. Zhao C, Zhang JC, Song JF (2001) Anal Biochem 297:170
31. Dekanski A, Stevanovic J, Stevanovic R, Jovanovic VM (2001) Carbon 39:1207
32. Zhu X, Gan X, Wang J, Chen T, Li G (2005) J Mol Catal A Chem 239:201
33. Ralph TR, Hitchman ML, Millington JP, Walsh FC (1994) J Electroanal Chem 375:1